Cholangiocyte-Derived Exosomal Long Noncoding RNA PICALM-AU1 Promotes Pulmonary Endothelial Cell EndMT in Hepatopulmonary Syndrome

Congwen Yang
Third Military Medical University Southwest Hospital Department of Anaesthesiology
Yihui Yang
The Third Affiliated Hospital of Zunyi Medical University
Yang Chen
Third Military Medical University Southwest Hospital Department of Anaesthesiology
Jian Huang
Third Military Medical University Southwest Hospital Department of Anaesthesiology
Caiyi Li
Third Military Medical University Southwest Hospital Department of Anaesthesiology
Dan Li
Third Military Medical University Southwest Hospital Department of Anaesthesiology
Xi Tang
Third Military Medical University Southwest Hospital Department of Anaesthesiology
Jiaoling Ning
Third Military Medical University Southwest Hospital Department of Anaesthesiology
Jianteng Gu
Third Military Medical University Southwest Hospital Department of Anaesthesiology
Bin Yi
Third Military Medical University Southwest Hospital Department of Anaesthesiology
kaizhi lu (lukaizhi2010@163.com)
Southwest Hospital, Third Military Medical University https://orcid.org/0000-0001-5160-9762

Research

Keywords: lncRNA, PICALM-AU1, EndMT, hepatopulmonary syndrome

Posted Date: November 15th, 2021

DOI: https://doi.org/10.21203/rs.3.rs-1054771/v1

Abstract

Background: Hepatopulmonary syndrome (HPS) is an important clinical problem with limited understanding of disease pathologies. Exosome mediated cell-cell communication can modulate various cellular functions by transferring a variety of intracellular components to target cells. A new lncRNA PICALM-AU1 was found and upregulated in the liver of subjects with HPS. However, the expression and biological functions of the lncRNA PICALM-AU1 are still unknown.

Methods: HPS rat model was constructed by common bile duct ligation (CBDL). RNA macroarray was used to analyze the expression differential lncRNAs in HPS rat liver. PICALM-AU1 expression in the serum exosome was measured in 56 HPS patients and in 73 patients with liver cirrhosis but not HPS. qPCR, Fluorescence in situ hybridization were used to analyze PICALM-AU1 expression and location. Virus derived PICALM-AU1 upregulation and down regulation were applied in rats and PMVECs cells. The effects of PICALM-AU1 on PMVECs was determined via CCK8 assay and transwell assay. PICALM-AU1 and miR144-3p relationship was analysis by Dual-luciferase reporter assay.

Results: In this study, we found lncRNA PICALM-AU1 expressed in the cholangiocyte of liver, secreted as exosome into the serum. PICALM-AU1 carrying serum exosomes induced endothelial-mesenchymal transition (EndMT) of PMVECs and promoted lung injury. Furthermore, overexpression of PICALM-AU1 significantly suppressed miR144-3p and subsequently induced ZEB1 expression.

Conclusions: Taken together, our findings present a road map of targeting the newly identified cholangiocyte-derived exosomal lncRNA PICALM-AU1 plays a critical role in the pathologic angiogenesis of HPS by promoting EndMT and represents a potential therapeutic target for HPS.

Introduction

Hepatopulmonary syndrome (HPS), characterized by hypoxemia and intrapulmonary shunting, occurs in 5 to 32% of patients with liver disease[1]. HPS significantly increases mortality and worsens functional status and quality of life in patients with cirrhosis[2]. Despite growing knowledge of the mechanisms involved in HPS development, its pathogenesis has not been fully unraveled[3–6].

Pulmonary angiogenesis plays a vital role in the HPS development[7]. Soluble molecules synthesized in pathological liver, such as the vascular endothelial growth factor (VEGF), bone morphogenic protein-2 (BMP2), BMP9, placental growth factor (PIGF). These pro-angiogenic factors was transported into the lung, functional as inducing gene expression and promoting pulmonary microvascular formation, thus aggravating the degree of respiratory distress in HPS[8–11]. Endothelial-mesenchymal transition (EndMT) is a process that is characterized by the loss of features of endothelial cells and acquisition of specific markers of mesenchymal cells, which plays a key role in regulating endothelial function, development and structural remodeling of myocardium, blood vessels and valves[12–14]. A large number of studies have implicated EndMT in the vascular diseases including cerebral cavemous malformations, pulmonary hypertension, vascular graft remodeling, tumorigenesis and atherosclerosis [15–19]. Chronic

obstructive lung disease (COPD) is caused by hypoxia or other hypoxia-independent stimuli- inducing pulmonary vascular remodeling. It reported that S100A4 expression was observed in remodeled intrapulmonary arteries of COPD patients, targeting S100A4 could serve as potential therapeutic option for prevention of vascular remodeling in COPD patients [20, 21]. However, the mechanism how EndMT regulated HPS pathology is largely unclear, although recent study indicates possible links with exosomes [22].

Exosomes, the small extracellular membrane-enclosed vesicles formed by the inward budding of endosomal member and released extracellularly via fusion with the plasma membrane. Exosomal cargos, including noncoding RNAs, proteins and lipids, are implicated in various disease [23, 24],[25],[26], Cholangiocyte-derived exosomal LncRNA H19 promotes hepatic stellate cell activation and cholestatic liver fibrosis[27, 28]. In our previous study, Lin found that hepatocyte-derived exosomal miR194 promotes PMVECs angiogenesis of HPS pulmonary[29]. This study preliminarily described that in HPS, exosomes secreted into serum, promoted pulmonary microvessels formation. However, except from microRNA, lncRNAs in exosomes also play an important regulatory role in physiological functions and pathological production. we mainly wanted to explore whether exosomes synthesized from the liver contained potentially important lncRNA, and to control HPS pathology through a long-distance regulation mechanism across organs.

Here, a novel lncRNA (MRAK138283, named PICALM-AU1) was identified by microarray screening in the HPS rat liver. We demonstrate that PICALM-AU1 is rich in cholangiocyte-derived exosomes of HPS rat liver. The quantity of PICALM-AU1 in serum exosomes is positive correlated to the severity of lung injury in rat HPS models and human HPS patients. Importantly, we find that cholangiocyte-derived exosome PICALM-AU1 is a key molecular to promote EndMT of PMVECs in HPS. It suggests that exosome derived lncRNA PICALMAU1 from HPS liver regulate lung injury. Furtherly, PICALM-AU1 can be used as a potential therapeutic target for HPS.

Materials And Methods

Animal model and treatments

Common bile duct ligation rat model (CBDL). The common bile duct ligation operation of rat is one of the typical HPS model with a well-established methodology[3, 30]. All animal experiments were approved by the Animal Care Committee of Third Military Medical University, Chongqing, China. Male Sprague-Dawley rats (200-220g, 6-7 weeks age, 30 rats each group) were anesthetized with intramuscular injections of ketamine (80mg/kg) and xylazine (10mg/kg). The control rat was sham-operated by isolation of the common bile duct without ligation. The lung of the animals was dissected and analyzed after 1 week, 3 week and 5 weeks after surgery. Blood sample was aseptically drawn from the abdominal aorta during laparotomy. A 0.2ml sample of arterial blood was collected into a heparinized gas capillary tube to measure the arterial gas levels. Serum was separated from the blood samples (centrifugation at 2000×g, 4°C), then was used to separate exosomes.

Arterial blood gas analysis and sample preparation. Arterial blood was collected from the abdominal aorta under chloral hydrate anesthesia (40 mg/kg IP, Nembutal, Ceva Sante Animale), and blood gas analysis was performed in the Laboratory of Clinical Biology (Southwest Hospital, China). Hypoxemia was defined as a PaO_2 < 80 mmHg. Additionally, serum was prepared by centrifugation of the blood at 10000 rpm for 10 min at 4°C and stored at −80°C prior to analysis.

Exosome treatment. To analysis the function of HPS exosome toward rat lung, exosomes isolated from sham rat serum, HPS rat serum, MIBECs cell line and MIBECs with PICALM-AU1 overexpression (method as described below) were injected into healthy rats (200-220g, 6-7 weeks age). Rats were randomly divided into four groups (ss-Exo, sham-serum exosome; Hs-Exo, HPS serum exosome; ct-Exo, MIBECs-derived Exo; PO-Exo, PICALM-AU1 OE MIBECs-derived exosome). Exosomes (100μg total protein in 100μL volume) were injected three times and once every other day via the caudal vein. Exosomes from sham and HPS rat serum were used to treat PMVECs to analysis EndMT in cell line.

Virus treatment. To analysis the function of PICALM-AU1 toward rat lung, lentivirus with PICALM-AU1 overexpression and knockdown was constructed. The LV-NC, LV-PICALM-OE and LV-PICALM-KD viruses were injected into healthy rats (200-220g, 6-7 weeks age) via caudal vein (each at 100μL of 2×10^{10}TU/ml). After two weeks, the rats were carried on CBDL operation; To investigate the function of exosomal-PICALM-AU1 toward rat lung, lentivirus LV-NC and LV-PICALM-OE were treated MIBECs (each at 10μL of 1×10^{9}TU/mL). After 72hr, detection of the PICALM-AU1 expression. And then, exosome was isolated for rat infection; To analysis the function of PICALM-AU1 toward PMVECs, LV-NC, LV-PICALM-OE and LV-PICALM-KD viruses were treated PMVECs (each at 10μL of 1×10^{9}TU/mL). After 72hr, detection of the gene expression, protein synthesis was carried on.

Microarray analysis

Total RNA of CBDL operation group and sham group rat liver was extracted and transcribed. Double-stranded cDNA was labeled using the Quick Amp Labeling Kit (Agilent Technologies Inc, USA) and hybridized to the Array star Rat 8×60K lncRNA Array, version 2.0. Following the washing steps, the arrays were scanned with the Agilent Scanner G2505B, and the array images were analyzed using Agilent Feature Extraction software, version 10.7.3.1. Quantile normalization and subsequent data processing were performed using GeneSpring GX software, version 11.5.1 (Agilent Technologies Inc, USA). Volcano plot filtering was used to identify the lncRNAs with statistically significant differences, and the threshold to screen upregulated or downregulated lncRNAs was identified at a fold change of 1.5 or greater and a P value of 0.05 or less.

Tissue harvest and Histology

Liver and lung samples were fixed in 4% phosphate buffered formaldehyde solution (Klinipath, Belgium), dehydrated, embedded in paraffin and stained with Hematoxylin and eosin, Masson staining, Immunohistochemistry, Immunofluorescence and Fluorescence in situ hybridization. All of the antibody information was as followed in Table S2.

H.E staining of rat lung tissue was according to previous study [3]. Immunohistochemical staining on lung tissue allowed to quantify protein expression levels. Specific anti-VWF, anti-VE-cadherin and anti-Vimentin were used. Slices that underwent immunostaining with omission of primary antibodies or with IgG were used as negative controls. Paraffin-embedded lung sections (5 μm thickness) were deparaffinized, rehydrated by serial immersion in ethanol, and pretreated with citrate buffer. Non-specific binding sites were blocked via incubation in 3% H_2O_2 (Merck, Germany) and BSA respectively. Epitope detection was performed using the ultraView Universal DAB Detection Kit (Dako, Denmark). Counterstaining was performed with hematoxylin.

The vascular density of specimens stained for VWF was measured semi-quantitatively using Cell Software (Olympus, Japan). Results are expressed as mean positively stained area (% ± SE) per field. The number of vascular per high power field (objective 40×) was counted in 15 randomly selected fields for each rat, and the mean value of the vascular in these fields was calculated (mean number of vascular per field ± SE). All final histological scores are represented as the mean of the scores determined by two independent researchers, who were blinded to the study samples.

Immunofluorescence. For immunofluorescent double staining, paraffin-embedded lung sections (5 μm thickness) or cell slides were deparaffinized, rehydrated by serial immersion in ethanol and pretreated with EDTA, followed by incubation in 50 mM NH_4Cl, 0.1% Triton X-100 and 1% BSA. Anti-VE-cadherin, anti-Vimentin, anti-ZEB1 and anti-ZO1 were used as primary antibodies. Slices that underwent immunostaining with omission of primary antibodies or with IgG were used as negative controls. The binding sites of the primary antibodies were revealed with Alexa Fluor-594 goat anti-rabbit and Alexa Fluor-488 goat anti-mouse secondary antibodies (Invitrogen, USA). Nuclei were stained with 4', 6-diamidino-2-phenylindole (DAPI) (Life Technologies, USA). Samples were visualized with a fluorescence microscope (Olympus, Japan).

FISH (Fluorescence in situ hybridization) combined with fluorescent IHC staining

FISH targeting PICALM-AU1 in rat liver tissue sections was performed using a commercially available RNA scope Multiplex Fluorescent Reagent Kit v2 (Advanced Cell Diagnostics, USA) by following the manufacturer's instruction. Fluorescent IHC staining target PICALM-AU1 was performed after FISH staining as described in the above section (Histopathology, Masson's Trichrome staining, and immunohistochemistry). Zeiss LSM 700 confocal laser scanning microscopy were used to visualize FISH results (Carl Zeiss, Germany).

cDNA synthesis and qPCR

LncRNA, miRNA and mRNA expression were analyzed in total RNA from tissue and cell samples using the Applied Biosystems 7000 sequence detection system (Applied Biosystems, UK) with SYBR Green and the comparative CT method. Values were reported relative to the endogenous control glyceraldehyde-3-

phosphate dehydrogenase. All amplification reactions were performed in three independent times. Primer sequences were described in Supplementary Table S1.

Western blot

Protein expression was determined by Western blot in rat lung and PMVECs samples as previously described [31]. Antibodies information was shown in Table S2. Blots were visualized by ECL reagents (DAKO, Denmark), and digital images were taken using a luminescent image analyzer LAS-4000 (General Electric, UK). β-actin was used for the normalization of quantitative densitometry values.

Cell culture and in vitro experiments

Rat pulmonary microvascular endothelial cells (PMVECs) and mice intrahepatic biliary epithelial cells (MIBECs) were purchased from American Type Culture Collection (ATCC Cell Biology Collection, USA). And cells were maintained at 37°C in RPMI medium (Gibco, USA) supplemented with 10% fetal bovine serum (Invitrogen, USA). For cell transfection experiments, cells were seeded at 60-70% confluence. Vectors were mixed with Lipofectamine 3000 (Promega, USA), diluted in EGM2, and treated for 24h, as described [31]. After 24h, cells were treated for miR144-3p mimics/ inhibitor or sham/HPS exosome. Then, Luc activity was detected by Dual-Luciferase Reporter Assay System (Promega, USA) in the GloMax-Multi Detection System Photometer (Promega, USA). Assays was carried out three times independently and the average Luc activity levels were presented as mean ± SE.

HPS patient specimens

We selected the HPS patients and collected the blood. Then, exosome was isolated for detecting gene transcript. This study was conducted according to the ethical guidelines of the Declaration of Helsinki. It was approved by the U.S. National Library of Medicine, Clinical Trails.gov (https://clinicaltrials.gov/, NCT:03435406). All participants provided written informed consent and agreed to the publication of their anonymous information. Patients were screened for the presence of HPS. HPS was diagnosed by three parameters: (1) presence of cirrhosis (2) positive contrast-enhanced echocardiography, and (3) an alveolar-arterial oxygen gradient (P(A-a) O_2) ≥ 15 mmHg (or ≥20 mmHg in patients >64 years). Intrapulmonary vascular dilations were assessed by contrast-enhanced echocardiography. Agitated saline causes microbubbles of >10 μm in diameter that usually do not pass through the pulmonary capillary bed. Appearance of microbubbles, after injecting in a peripheral vein, first in the right heart, and within three to six heart actions in the left heart demonstrates abnormal vasodilation of the intrapulmonary capillary bed. Early (<3 heart beats) appearance of microbubbles in the left heart was considered as intracardiac shunting. These patients were excluded from this study as the presence or absence of intrapulmonary shunting could not be judged by contrast-enhanced echocardiography.

Exosome Isolation and characterization

Human patient serum, rat serum and MIBECs medium were collected by centrifugation at 2,000 g for 15 min followed by 16,000 g for 20 min at 4°C. Then, the supernatants were collected and ultracentrifuged at 110,000 g for 70 min. Afterwards, pellets were resuspended in sterile PBS and purified by centrifugation

at 110,000 g for 1h. Subsequently, the exosomes were resuspended in PBS and filtered through 0.22 μm filter (Millipore, USA), stored at -80°C for further analysis.

To characterize the morphology of the isolated exosomes, transmission electron microscopy (Hitachi HT7700, Japan) was used. For size distribution of the isolated exosomes, qNano (Izon Science, New Zealand) was used following the manufacturer's instructions. To analyze the protein markers of exosomes, Western blotting assays were performed, and anti-CD63, anti-CD86 antibodies were used.

Statistical analysis

Results were obtained from at least three independent experiments and are expressed as mean±SD. Data were analyzed by two-tailed student t test, one way-variance analysis with Tukey's post-hoc test or linear regression using GraphPad Prism software version 8.0 (GraphPad Software Inc., USA). A P value of ≤ 0.05 was considered statistically significant.

Results

LncRNA PICALM-AU1 is highly expressed in the HPS liver

To identify a key lncRNA regulating HPS progress, we constructed the HPS rat model by CBDL (Fig. 1A). The CBDL rat was cirrhosis, low efficiency of pulmonary gas exchange and there was excessive angiogenesis of pulmonary micro-vessels. RNA sequencing was performed to compare CBDL rat liver and sham rat liver RNA expression. After filtering data for long noncoding RNA annotation, expression levels, there were 88 lncRNAs upregulated and 10 lncRNAs downregulated after the CBDL operation (Fig. 1BC). Top 4 upregulated lncRNAs was selected as a primary target. qPCR showed that MRAK138283 was mostly upregulated in the early pathological phage of CBDL rat liver (Fig. 1E). So, we choose MRAK138283 (NCBI: LOC102550036) to further study. It is a new lncRNA that has not been reported. And MRAK138283 is located in the antisense strand of rat chromosome 1. It is also in the upstream of Picalm gene. So, we named this lncRNA as "PICALM-AU1". And it has two exons with 368bp in fully CDS (Fig. 1D).

Furtherly, we analyzed PICALM-AU1 expression in the different period of sham and CBDL operation rat liver. The result showed PICALM-AU1 level is the highest in the liver (Fig. 1F). In HPS rat liver, it expressed dramatically high in the 1st week and the expression increases with time (Fig. 1E).

PICALM-AU1 synthesized on Cholangiocytes and secreted into serum as exosome

To determine the expression pattern, we first examined PICALM-AU1 expression in the sham and HPS rat liver by FISH staining. The result showed PICALM-AU1 expression was higher in HPS rat liver than that of sham and located in CK19-positive cholangiocytes in 3-week CBDL rat (Fig. 2A). Then, we separated three main type of cells in liver, Cholangiocyte cells, Kupffer cells and Hepatocyte cells, to detect whether PICALM-AU1 was synthesis in cholangiocyte cell. qPCR showed PICALM-AU1 mRNA was highly and

predominantly expressed in cholangiocytes, rather than other two type of cells. And PICALM-AU1 levels in HPS group were 30% higher than that of sham group (Fig. 2B). FISH staining of Cholangiocyte cell showed PICALM-AU1 mainly located in the cytoplasm, also in nuclear (Fig. 2C).

Given that PICALM-AU1 is expressed mainly in the cholangiocytes of liver and located in the cytoplasm, we proposed that that PICALM-AU1 may secreted from liver cholangiocytes as exosome and functions in the lung. So, we isolated Sham, HPS rat exosome and detected the expression trend of PICALM-AU1 (Fig. 2D). Correlation analysis showed that hepatic PICALM-AU1 mRNA levels were positively correlated with that of serum exosome (Fig. 2E, left side). Furthermore, IHC staining of CD63, a surface marker for exosomes, indicated that CD63 was expressed and up-regulated in cholangiocytes (Fig. 2A, lower line). These results indicated that PICALM-AU1 expressed in Cholangiocytes and secreted into serum as exosome for function.

Levels of serum exosomal PICALM-AU1 are correlated with the severity of HPS in Rat model and human patients

To identify the function of exosomal PICALM-AU1 in pathological angiogenesis of HPS, the relation between PICALM-AU1 and HPS rat gas exchange was discussed. Correlation analysis showed PICALM-AU1 in exosome were positively correlated with carbon dioxide (PCO_2), negatively with partial pressure of partial pressure of oxygen (PO_2) (Fig. 2E, middle and right side).

To confirm the result, a total of 56 HPS patients from chronic cirrhosis and 73 control chronic cirrhosis patients with not HPS were used in this study. From the basic information, HPS patients had vertical dyspnea and positive of Type-B ultrasonic. HPS patients had higher partial pressure of carbon dioxide in artery, and lower partial pressure of oxygen in artery than that of no HPS patients (Table 1). HPS patient serum exo-PICALM-AU1 levels was significantly highly than that of no HPS patients (Fig. 2F, left side). And serum exosomal PICALM-AU1 levels were also negatively correlated with PO_2, but positively correlated with PCO_2 (Fig. 2F, middle and right side). It indicates that serum exosomal PICALM-AU1 is associated with HPS pathological formation and development.

Exo-PICALM-AU1 promoted PMVECs EndMT in rat lung

PMVECs EndMT plays an important role in regulating angiogenesis and blood vessel remodeling [32]. Firstly, immunohistochemisty and Western blot were employed to confirm the function of EndMT in HPS lung. Endothelia biomarker VE-cadherin and mesenchyme cell biomarker Vimentin expression during the HPS progression were detected. Results showed that VE-cadherin expression was reduced and Vimentin expression was induced in the rat lung during the HPS period (Fig.S1AB). The data suggested that EndMT is occurs in pathologic pulmonary micro-vascular angiogenesis.

To identify whether exosome-derived PICALM-AU1 stimulated PMVECs EndMT in vivo, we used HPS rat derived exosome treated normal rat. For confirm PICALM-AU1 function, exosome from MIBECs cell line and MIBECs with PICALM-AU1 overexpression were also treated normal rat. The strategy was

demonstrated in Fig. 3A. qPCR detected EndMT related genes expression. VE-cadherin mRNA transcription in HPS rat derived exosome treatment was reduced to 35% than that of sham-serum exosome treatment. And VE-cadherin mRNA level in PICALM-AU1 over expression MIBECs derived exosome treatment was reduced to 45% than that of control exosome treatment. Instead, *Vimentin*, TGFβ and collagen1 mRNA transcription has a significant induction after HPS rat exosome treatment or PICALM-AU1 over expression (Fig. 3B). Moreover, Immunohistochemical staining confirmed that VE-cadherin expression was reduced by HPS rat derived exosome treatment and PICALM-AU1 over expression MIBECs derived exosome treatment. However, Vimentin expression trend was opposite with that of VE-cadherin (Fig. 3C).

Then, to investigate whether or not EndMT of lung PMVECs is induced by PICALM-AU1, CBDL rat was treated by PICALM-AU1 over expression or PICALM-AU1 knockdown with Adeno-associated virus. The experiment strategy was as illustrated in Fig. 3D. The pathological changes of rats were more serious and VE-cadherin mRNA transcription and protein expression was reduced in the PICALM-AU1 over expression virus rat control to HPS group or sham group. However, Vimentin expression trend was opposite with that of VE-cadherin. And PICALM-AU1 knockdown virus treatment could partially reverse the HPS pathology and the relative genes synthesis (Fig. 3EF).

To confirm that Exo-PICALM-AU1 can promote PMVECs EndMT in vitro, we firstly used exosome from HPS rat serum and exosome from MIBECs (which is over expressed PICALM-AU1 in MIBECs cell line by lentivirus) treated PMVECs. PMVECs proliferation and migration was both induced by HPS exosome and MIBECs derived exosome, which over expressed PICALM-AU1 (Fig. 4ABC). And Adeno-associated virus with PICALM-AU1 overexpression, also induce PMVECs proliferation and migration. However, adeno-associated virus with PICALM-AU1 knockdown could inhibit PMVECs proliferation and migration (Fig. 4DEF). All of the results suggested that serum exosomal PICALM-AU1 induced HPS rat lung PMVECs EndMT and promoted HPS pathological progression in rats.

miR144-3p is one of the PICALM-AU1 targets

To investigate how PICALM-AU1 regulated PMVECs EndMT, we first analyzed the gene expression network in HPS lung by microarray (data unpublished). And we found microRNA 144-3p is a putative target of PICALM-AU1 (Fig.S2). There is a miR144-3p binding site on PICALM-AU1 sequence (Fig. 6C). In our previous study, we found miR144-3p can inhibit PMVECs cell proliferation in HPS lung [3]. This information indicated that PICALM-AU1 may regulate PMVECs EndMT by miR144-3p.

To confirm the relationship between PICALM-AU1 and miR144-3p, HPS rat model, exosome treatment rat model and recombinant adeno-associated virus mediated PICALM-AU1 over expression/ knockdown in HPS rats were used to treat HPS rat. In HPS rat model, the expression trend of miR144-3p decreased rapidly with HPS development. And the expression trend is opposite to that of PICALM-AU1 (Fig. 5A). In exosome treatment rat model, miR144-3p was reduced by HPS rat serum exosome treated. And miR144-3p expression level was also opposite to that of PICALM-AU1 (Fig. 5B). The result is also confirmed in the recombinant adeno-associated virus treatment rat model. When PICALM-AU1 overexpression, miR144-3p

mRNA level was reduced. When PICALM-AU1 knockdown, miR144-3p mRNA level was induced (Fig. 5C). The result showed miR144-3p is a potential target of PICALM-AU1, and the expression trend was negatively correlated with that of PICALM-AU1 in HPS rat lung.

PICALM-AU1 inhibited miR144-3p

Firstly, to identify whether miR144-3p can regulate EndMT of PMVECs, we used miR144-3p mimics and inhibitor respective to treat PMVECs. Immunofluorescence showed that over expression of miR144-3p could promote EndMT by inducing Vimentin expression and reducing VE-cadherin expression. And reduction of miR144-3p inhibited EndMT by suppressing Vimentin expression. (Fig. 6AB).

Then, to analyze the regulation function of PICALM-AU1 to miR144-3p, we constructed a luciferase reporter system (Fig. 6C). The psiCHECK2 vector with Tie2 3'UTR (with miR144-3p binding sites, reported in our previous work [3]) downstream of the LUC gene was transfected into the PMVECs line. Then, miR144-3p mimic and inhibitor were used to treat PMVECs to upregulate and downregulate miR144-3p level in cells. And nuclear fragment of PICALM-AU WT and PICALM-AU1 MUT was used to overexpress PICALM-AU1 level in cells. When mutated PICALM-AU1 nuclear fragment was transfected into PMVECs, miR144-3p mimic reduced LUC activity to 20% and miR144-3p inhibitor induced LUC activity by 1.5-folds. When wildtype PICALM-AU1 nuclear fragment was transfected into PMVECs, the reduction of LUC activity by miR144-3p mimics was recovered. And the LUC activity reached the maximum in miR144-3p inhibitor treated PMVECs (Fig. 6D). This means that PICALM-AU1 is negatively regulating miR144-3p level in PMVECs.

To confirm this result, we used PICALM-AU1 overexpression and knockdown lentivirus treated PMVECs. Luciferase assay showed that PICALM-AU1 over expression could induce the Luc activity by 1.6-folds. However, PICALM-AU1 knockdown could reduce the Luc activity to 25% (Fig. 6E). These results suggested that PICALM-AU1 can regulate PMVECs EndMT by inhibit miR144-3p level.

miR144-3p inhibited PMVECs EndMT by ZEB1 transcriptional factor

To analyze the role of miR144-3p in regulating EndMT, the target regulated genes were predicted by miRWalk and miRtarBase websites (http://mirwalk.umm.uni-heidelberg.de/, http://mirtarbase.mbc.nctu.edu.tw/php/index.php. We found that ZEB1 is one of the miR144-3p putative target gene (Table S3). ZEB1, full name is Zinc Finger E-Box Binding Homeobox 1, acts as a transcriptional repressor inhibits interleukin-2 (IL-2) gene expression[33]. It also represses E-cadherin promoter and induces an epithelial-mesenchymal transition (EMT) by recruiting SMARCA4/BRG1 [33–35]. So, we firstly overexpressed or knocked down miR144-3p by specific mimics and inhibitor, and detected ZEB1, SNAIL, TWIST and SLUG gene transcript by qPCR. The result showed that ZEB1 gene transcript in PMVECs cell were reduced by miR144-3p mimics treatment, and were induced by miR144-3p inhibitor treatment (Fig. 6F). Then, we overexpressed or knocked down PICALM-AU1 in PMVECs cell line. The result showed ZEB1 gene transcript in PMVECs cell was induced when PICALM-AU1 was

overexpressed, and was reduced by PICALM-AU1 knockdown (Fig. 6G). Then, we used dual Luciferase assay to analyze the miR144-3p mediated regulation of ZEB1. The vector with ZEB1 3'UTR was transfected into PMVECs and the cell line treated with miR144-3p mimics and miR144-3p inhibitor. The result showed miR144-3p can bind with ZEB1 3'UTR and inhibit Luciferase activity. When the binding site was broken, miR144-3p could not inhibit Luciferase activity anymore (Fig. 6H). We furtherly overexpressed PICALM-AU1 based on the dual Luciferase assay in PMVECs, and this could partially recovery Luciferase activity by miR144-3p inhibition (Fig. 6I). These results showed that miR144-3p can inhibit PMVECs EndMT via ZEB1, and PICALM-AU1 can promote EndMT by inhibit miR144-3p.

PICALM-AU1 promoted PMVECs EndMT by miR144-3p/ZEB1

To identify whether or not PICALM-AU1 regulates PMVECs EndMT by miR144-3p/ZEB1, PMVECs were treated with sham rat serum exosome and HPS rat serum exosome. Immunofluorescence, qPCR and Western blot showed that ZEB1 expression was induced and VE-cadherin, N-cadherin and ZO-1 expression were reduced after HPS exo treatment than that of sham exo treatment (Fig. 7ABC). And then, PICALM-AU1 overexpression and knockdown were achieved by recombinant adeno associated virus. IF, qPCR and Western blot showed that ZEB1 expression was induced and VE-cadherin, ZO-1 expression were reduced after PICALM-AU1 over expression than that of control. And ZEB1 expression was reduced and VE-cadherin, ZO-1 expression was induced after PICALM-AU1 knockdown than that of control (Fig. 7DEF). These results showed that PICALM-AU1, which is synthetized from liver cholangiocytes and secreted into exosome and functioned in HPS lung, promoted PMVECs EndMT by miR144-3p/ZEB1.

Discussion

In previous studies, we focus more attention on the mechanism of pulmonary microvascular remodeling and how to block it to improve HPS pathology[10, 36–40]. However, the effect is limited. Then we think, the pathological of HPS is come from liver disease. So, the secretion of liver is the key factor to make HPS development. In our recently study, we found a c-kit$^+$ cell was collected into lung by serum SDF1 which may participate in angiogenesis of pulmonary microvascular [5]. In this study, we found a long noncoding RNA, PICALM-AU1, expressed mainly in cholangiocytes of liver, secreted as exosome. We show that cholangiocyte derived lncRNA PICALM-AU1 plays a pivotal role in activating PMVECs EndMT and promoting HPS excessive angiogenesis.

lncRNA PICALM-AU1 is a new detected lncRNA. It has two exons with 368bp in fully CDS. Under normal physiological condition, PICALM-AU1 expression has a low level in all tissues. However, PICALM-AU1 level was dramatic induced in the liver and lung of HPS rat. And in this study, we can identify that cholangiocytes are the primary source of hepatic PICALM-AU1 under both physiologic and cholestatic conditions by using three different approaches, including immunopurification of primary cholangiocytes, laser capture microdissection, and FISH-IHC assay.

Exosomal PICALM-AU1 has a critical rule in the pathological angiogenesis of HPS rat lung. Exosomes are small extracellular vehicles released by various types of cells, which can carry multiple cargos, including protein, DNA, mRNA, lncRNA and lipids [41–43]. Recently, exosomes have drawn significant attention as essential mediators of intercellular communication under both physiological and pathological conditions [44]. We think, EndMT is a core factor for contribute to the accumulation of pulmonary microvascular formation, recapitulating pathways associated with HPS development. Importantly, EndMT may be reversible [45, 46]. Thus, insights into the mechanisms controlling EndMT are relevant to vascular remodeling and are important to develop the new therapies aimed at reversing vascular remodeling to relieve the pain of HPS patients. This article is focused on the characteristics, functions and roles of EndMT in HPS vascular remodeling.

In summary, this study explored roles of PICALM-AU1 in regulating EndMT of HPS pathological blood vessel remolding by exosome mediated communication between distant organs. This study implicates future clinical perspective of exo-PICALM-AU1 signaling for the therapeutics after severe liver injuries.

Abbreviations

HPS, Hepatopulmonary Syndrome; EndMT, Endothelial stromal transformation; PMVECs, pulmonary microvascular endothelial cells; MIBECs, mice intrahepatic biliary epithelial cells; OE, Over expression; KD, knowck down; ss-Exo, serum of sham rat derived exosome; Hs-Exo, serum of HPS rat derived exosome; ct-Exo, control of MIBECs derived exosome; PO-Exo, PICALM-AU1 Over expression MIBECs-derived exosome

Declarations

Acknowledgements

Not applicable.

Authors' contributions

CY, BY and KL conceived the study concept and experimental design. CY, YY, YC and DL performed experiments, CL and JH collected data and performed statistical analysis, XT, JG and JN provided intellectual input and supervision. CY and DL drafted the manuscript. All authors read and approved the final manuscript.

Funding

This project was supported by the National Natural Science Foundation of China (81800060, 81671961, 81700046) and Natural Science Foundation of Chongqing, China (cstc2020jcyj-msxmX0361).

Conflict of interest

The authors declare that they have no conflict of interest.

Data Availability

The data that support the findings of the present study are available from the corresponding author upon reasonable request.

Consent for publication

Not applicable.

Competing interests

None

References

1. Rodriguez-Roisin R, Krowka MJ: **Hepatopulmonary syndrome–a liver-induced lung vascular disorder**. *N Engl J Med* 2008, **358**:2378–2387.
2. Fallon MB, Krowka MJ, Brown RS, Trotter JF, Zacks S, Roberts KE, Shah VH, Kaplowitz N, Forman L, Wille K, Kawut SM: **Impact of hepatopulmonary syndrome on quality of life and survival in liver transplant candidates**. *Gastroenterology* 2008, **135**:1168–1175.
3. Yang C, Lv K, Chen B, Yang Y, Ai X, Yu H, Yang Y, Yi B, Lu K: **miR144-3p inhibits PMVECs excessive proliferation in angiogenesis of hepatopulmonary syndrome via Tie2**. *Exp Cell Res* 2018, **365**:24–32.
4. Lejealle C, Paradis V, Bruno O, de Raucourt E, Francoz C, Soubrane O, Lebrec D, Bedossa P, Valla D, Mal H, et al: **Evidence for an association between intrahepatic vascular changes and the development of hepatopulmonary syndrome**. *Chest* 2018, **155**:123–136.
5. Shen CC, Chen B, Gu JT, Ning JL, Zeng J, Yi B, Lu KZ: **AMD3100 treatment attenuates pulmonary angiogenesis by reducing the c-kit (+) cells and its pro-angiogenic activity in CBDL rat lungs**. *Biochim Biophys Acta* 2017, **1864**:676–684.
6. Shen CC, Chen B, Gu JT, Ning JL, Chen L, Zeng J, Yi B, Lu KZ: **The angiogenic related functions of bone marrow mesenchymal stem cells are promoted by CBDL rat serum via the Akt/Nrf2 pathway**. *Experimental Cell Research* 2016, **344**:86–94.
7. Zhang J, Luo B, Tang L, Wang Y, Stockard CR, Kadish I, Van Groen T, Grizzle WE, Ponnazhagan S, Fallon MB: **Pulmonary angiogenesis in a rat model of hepatopulmonary syndrome**. *Gastroenterology* 2009, **136**:1070–1080.
8. Raevens S, Geerts A, Paridaens A, Lefere S, Verhelst X, Hoorens A, Van DJ, Maes T, Bracke KR, Casteleyn C: **Placental growth factor inhibition targets pulmonary angiogenesis and represents a novel therapy for hepatopulmonary syndrome in mice**. *Hepatology* 2017, **68**:634–651.
9. Liu C, Gao J, Chen B, Chen L, Belguise K, Yu W, Lu K, Wang X, Yi B: **Cyclooxygenase-2 promotes pulmonary intravascular macrophage accumulation by exacerbating BMP signaling in rat experimental hepatopulmonary syndrome**. *Biochem Pharmacol* 2017, **138**:205–215.

10. Liu C, Chen L, Zeng J, Cui J, Ning JN, Wang GS, Belguise K, Wang X, Qian GS, Lu KZ: **Bone morphogenic protein-2 regulates the myogenic differentiation of PMVECs in CBDL rat serum-induced pulmonary microvascular remodeling**. *Experimental Cell Research* 2015, **336**:109–118.
11. Fischer C, Jonckx B, Mazzone M, Zacchigna S, Loges S, Pattarini L, Chorianopoulos E, Liesenborghs L, Koch M, De Mol M, et al: **Anti-PlGF inhibits growth of VEGF(R)-inhibitor-resistant tumors without affecting healthy vessels**. *Cell* 2007, **131**:463–475.
12. Li Y, Lui KO, Zhou B: **Reassessing endothelial-to-mesenchymal transition in cardiovascular diseases**. *Nat Rev Cardiol* 2018, **15**:445–456.
13. Man S, Sanchez Duffhues G, Ten Dijke P, Baker D: **The therapeutic potential of targeting the endothelial-to-mesenchymal transition**. *Angiogenesis* 2019, **22**:3–13.
14. Xiao L, Dudley AC: **Fine-tuning vascular fate during endothelial-mesenchymal transition**. *J Pathol* 2017, **241**:25–35.
15. Wesseling M, Sakkers TR, Jager SCAD, Pasterkamp G, Goumans MJ: **The morphological and molecular mechanisms of epithelial/endothelial-to-mesenchymal transition and its involvement in atherosclerosis**. *Vascul Pharmacol* 2018, **106**:1–8.
16. Takada S, Hojo M, Tanigaki K, Miyamoto S: **Contribution of Endothelial-to-Mesenchymal Transition to the Pathogenesis of Human Cerebral and Orbital Cavernous Malformations**. *Neurosurgery* 2017, **81**:176–183.
17. Coll-Bonfill N, Musri MM, Ivo V, Barberã JA, Tura-Ceide O: **Transdifferentiation of endothelial cells to smooth muscle cells play an important role in vascular remodelling**. *Am J Stem Cells* 2016, **4**:13–21.
18. Cooley BC, Jose N, Jason M, Dan Y, Cynthia SH, Alejandra N, Fang F, Guibin C, Hong S, Walts AD: **TGF-β signaling mediates endothelial-to-mesenchymal transition (EndMT) during vein graft remodeling**. *Science Translational Medicine* 2014, **6**:227ra234.
19. Clere N, Renault S, Corre I: **Endothelial-to-Mesenchymal Transition in Cancer**. *Front Cell Dev Biol* 2020, **8**:747.
20. Sohal SS: **Endothelial to mesenchymal transition (EndMT): an active process in Chronic Obstructive Pulmonary Disease (COPD)**? *Respir Res* 2016, **17**:20.
21. Reimann S, Fink L, Wilhelm J, Hoffmann J, Bednorz M, Seimetz M, Dessureault I, Troesser R, Ghanim B, Klepetko W, et al: **Increased S100A4 expression in the vasculature of human COPD lungs and murine model of smoke-induced emphysema**. *Respir Res* 2015, **16**:127.
22. Visan KS, Lobb RJ, Moller A: **The role of exosomes in the promotion of epithelial-to-mesenchymal transition and metastasis**. *Front Biosci (Landmark Ed)* 2020, **25**:1022–1057.
23. Devhare PB, Ray RB: **Extracellular vesicles: Novel mediator for cell to cell communications in liver pathogenesis**. *Mol Aspects Med* 2017, **60**:115–122.
24. Masyuk AI, Masyuk TV, Larusso NF: **Exosomes in the pathogenesis, diagnostics and therapeutics of liver diseases**. *J Hepatol* 2013, **59**:621–625.

25. Loyer X, Zlatanova I, Devue C, Yin M, Howangyin KY, Klaihmon P, Guerin CL, Kheloufi M, Vilar J, Zannis K, et al: **Intra-Cardiac Release of Extracellular Vesicles Shapes Inflammation Following Myocardial Infarction**. *Circ Res* 2018, **123**:100–106.
26. Zeng Z, Li Y, Pan Y, Lan X, Song F, Sun J, Zhou K, Liu X, Ren X, Wang F, et al: **Cancer-derived exosomal miR-25-3p promotes pre-metastatic niche formation by inducing vascular permeability and angiogenesis**. *Nat Commun* 2018, **9**:5395–5408.
27. Li X, Liu R, Huang Z, Gurley EC, Wang X, Wang J, He H, Yang H, Lai G, Zhang L, et al: **Cholangiocyte-derived exosomal long noncoding RNA H19 promotes cholestatic liver injury in mouse and human**. *Hepatology* 2018.
28. Liu R, Li X, Zhu W, Wang Y, Zhao D, Wang X, Gurley EC, Liang G, Chen W, Lai G, et al: **Cholangiocyte-Derived Exosomal Long Noncoding RNA H19 Promotes Hepatic Stellate Cell Activation and Cholestatic Liver Fibrosis**. *Hepatology* 2019, **70**:1317–1335.
29. Chen L, Han Y, Li Y, Chen B, Bai X, Belguise K, Wang X, Chen Y, Yi B, Lu K: **Hepatocyte-derived exosomal MiR-194 activates PMVECs and promotes angiogenesis in hepatopulmonary syndrome**. *Cell Death Dis* 2019, **10**:853.
30. Yang Y, Chen B, Chen Y, Zu B, Yi B, Lu K: **A comparison of two common bile duct ligation methods to establish hepatopulmonary syndrome animal models**. *Lab Anim* 2015, **49**:71–79.
31. Yang C, Lin Y, Liu H, Shen G, Luo J, Zhang H, Peng Z, Chen E, Xing R, Han C, Xia Q: **The Broad Complex isoform 2 (BrC-Z2) transcriptional factor plays a critical role in vitellogenin transcription in the silkworm Bombyx mori**. *Biochim Biophys Acta* 2014, **1840**:2674–2684.
32. Welch-Reardon KM, Wu N, Hughes CC: **A role for partial endothelial-mesenchymal transitions in angiogenesis?** *Arterioscler Thromb Vasc Biol* 2015, **35**:303–308.
33. Williams TM, Moolten D, Burlein J, Romano J, Bhaerman R, Godillot A, Mellon M, Rauscher FJ, Kant JA: **Identification of a zinc finger protein that inhibits IL-2 gene expression**. *Science* 1991, **254**:1791–1794.
34. Cooley BC, Nevado J, Mellad J, Yang D, St. Hilaire C, Negro A, Fang F, Chen G, San H, Walts AD: **TGF-b Signaling Mediates Endothelial-to-Mesenchymal Transition (EndMT) During Vein Graft Remodeling**. *Science Translational Medicine* 2014, **6**:227–234.
35. Sánchez-Tilló E, Lázaro A, Torrent R, Cuatrecasas M, Vaquero EC, Castells A, Engel P, Postigo A: **ZEB1 represses E-cadherin and induces an EMT by recruiting the SWI/SNF chromatin-remodeling protein BRG1**. *Oncogene* 2010, **29**:3490–3500.
36. Xu D, Gu JT, Yi B, Chen L, Wang GS, Qian GS, Lu KZ: **Requirement of miR-9-dependent regulation of Myocd in PASMCs phenotypic modulation and proliferation induced by hepatopulmonary syndrome rat serum**. *Journal of Cellular & Molecular Medicine* 2015, **19**:2453–2461.
37. Chang CC, Wang SS, Hsieh HG, Lee WS, Chuang CL, Lin HC, Lee FY, Lee SD, Huang HC: **Rosuvastatin improves hepatopulmonary syndrome through inhibition of inflammatory angiogenesis of lung**. *Clin Sci (Lond)* 2015, **129**:449–460.

38. Yi B: **Annexin A1 protein regulates the expression of PMVEC cytoskeletal proteins in CBDL rat serum-induced pulmonary microvascular remodeling**. *Journal of Translational Medicine* 2013, **11**:98–106.
39. Jing Z, Yi B, Zhi W, Ning J, Wang X, Lu K: **Effect of annexin A2 on hepatopulmonary syndrome rat serum-induced proliferation of pulmonary arterial smooth muscle cells**. *Respiratory Physiology & Neurobiology* 2013, **185**:332–338.
40. Yi B, Cui J, Ning J, Gu J, Wang G, Bai L, Qian G, Lu K: **cGMP-dependent protein kinase Iα transfection inhibits hypoxia-induced migration, phenotype modulation and annexins A1 expression in human pulmonary artery smooth muscle cells**. *Biochemical & Biophysical Research Communications* 2012, **418**:598–602.
41. Kojima M, Gimenes-Junior JA, Langness S, Morishita K, Lavoie-Gagne O, Eliceiri B, Costantini TW, Coimbra R: **Exosomes, not protein or lipids, in mesenteric lymph activate inflammation: Unlocking the mystery of post-shock multiple organ failure**. *J Trauma Acute Care Surg* 2017, **82**:42–50.
42. Javeed N, Mukhopadhyay D: **Exosomes and their role in the micro-/macro-environment: a comprehensive review**. *The Journal of Biomedical Research* 2017, **30**:386–394.
43. Shashi B, Jan P, Shiv M, Donna C, Ivan L, Jeanine W, Hawau A, Karen K, Gyongyi S: **Circulating microRNAs in exosomes indicate hepatocyte injury and inflammation in alcoholic, drug-induced, and inflammatory liver diseases**. *Hepatology* 2012, **56**:1946–1957.
44. Kilchert C, Wittmann S, Vasiljeva L: **The regulation and functions of the nuclear RNA exosome complex**. *Nat Rev Mol Cell Biol* 2016, **17**:227–239.
45. Okada H, Kalluri R: **Recapitulation of kidney development paradigms by BMP-7 reverses chronic renal injury**. *Clinical & Experimental Nephrology* 2005, **9**:100–101.
46. Hirokazu O, Raghu K: **Cellular and molecular pathways that lead to progression and regression of renal fibrogenesis**. *Current Molecular Medicine* 2005, **5**:467–474.

Tables

Due to technical limitations, table 1 is only available as a download in the Supplemental Files section.

Figures

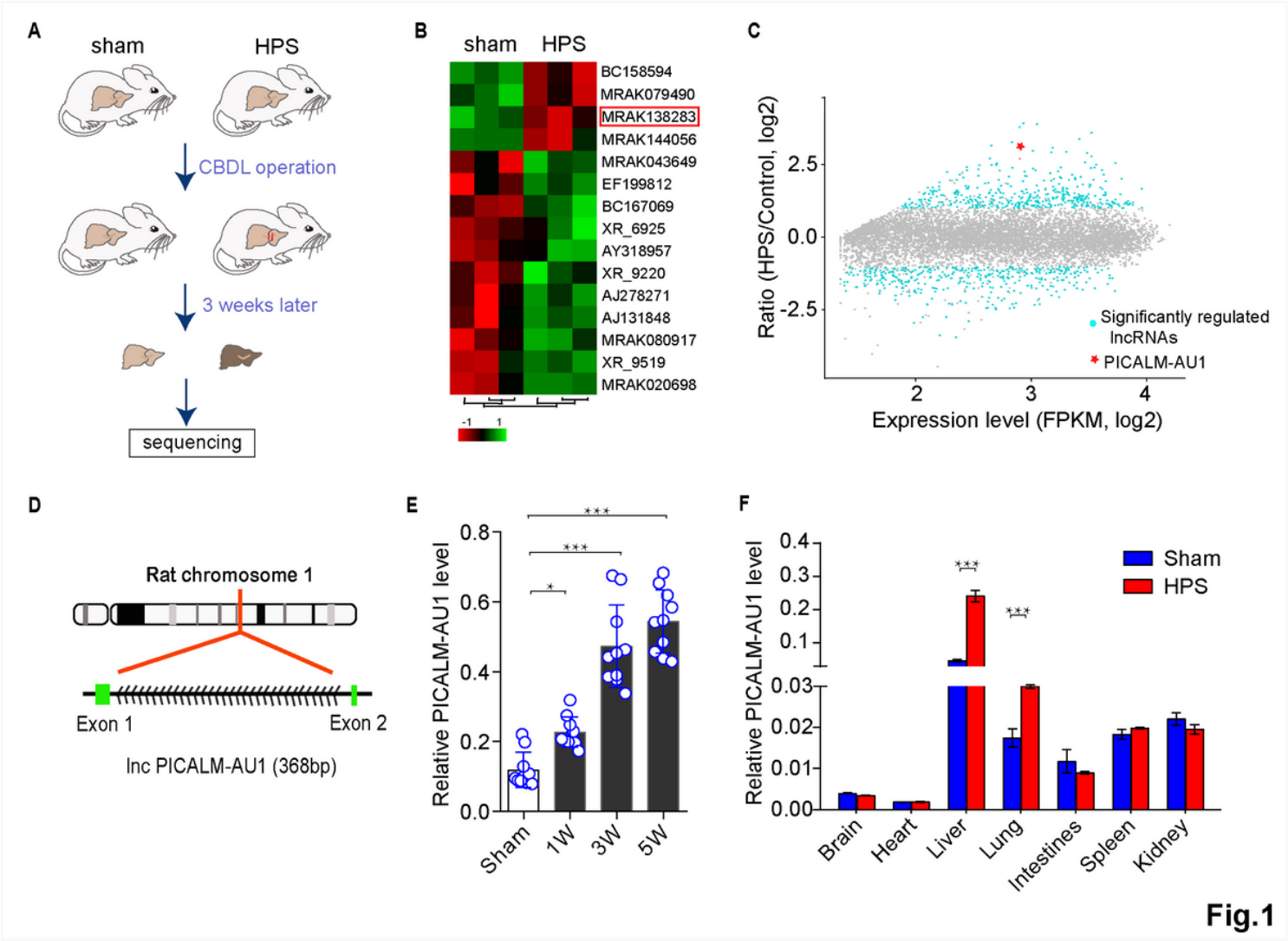

Figure 1

lncRNA PICALM-AU1 was highly expressed in the HPS liver (A) Strategy of Common bile duct ligation rat model construction. (B) Gene expression changes were assayed by deep sequencing of RNA Array. (C) Significantly regulated lncRNAs are highlighted in light blue, PICALM-AU1 is highlighted in red. (D) The structure and location of PICALM-AU1 in rat genomic chromosome. (E-F) qPCR analysis of PICALM-AU1 expression in the different stage of HPS rat liver and in different tissues at the third week of HPS rats. Statistical significance relative to sham group, *P < 0.05, **P < 0.01, ***P < 0.001, n = 10, t test.

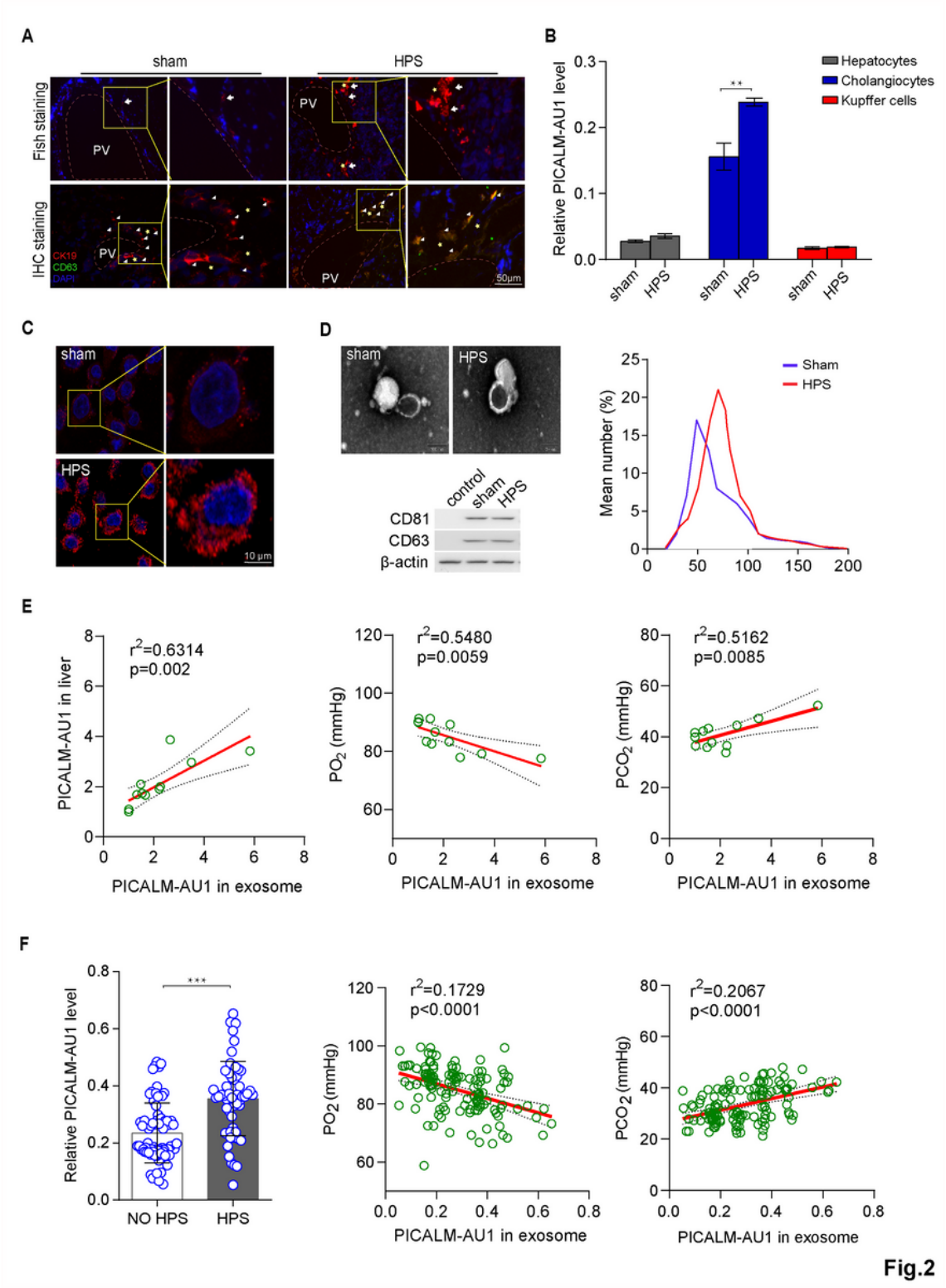

Fig.2

Figure 2

PICALM-AU1 expressed in the cholangiocyte and released as exosome (A) Representative images of FISH targeting PICALM-AU1 in liver are shown in upper line. Representative images of immunofluorescence targeting CK19 and CD63 are shown in lower line. Colocalization of CK19 and CD63 are indicated by white triangles. bile duct, yellow *; Portal vein, PV. (B) qPCR analysis PICALM-AU1 expression in the cholangiocytes, primary hepatocytes and Kupffer cells. (C) Subcellular localization of PICALM-AU1 in

cholangiocyte cell by FISH staining. (D) sham and HPS rat serum exosome were isolated and detected by the TEM (upper line) and Western blot (lower line), and the number of exosomes were analyzed (right). (E) Correlation between hepatic PICALM-AU1 and serum exosomal PICALM-AU1 (left), PO2 and exosomal PICALM-AU1 (middle), PCO2 and exosomal PICALM-AU1 (right) was analyzed. (F) exosomal PICALM-AU1 expression was analyzed in 56 HPS patients and 73 chronic liver patients without HPS (left). The correlation between PO2 and exosomal PICALM-AU1 (middle), PCO2 and exosomal PICALM-AU1 was analyzed (right).

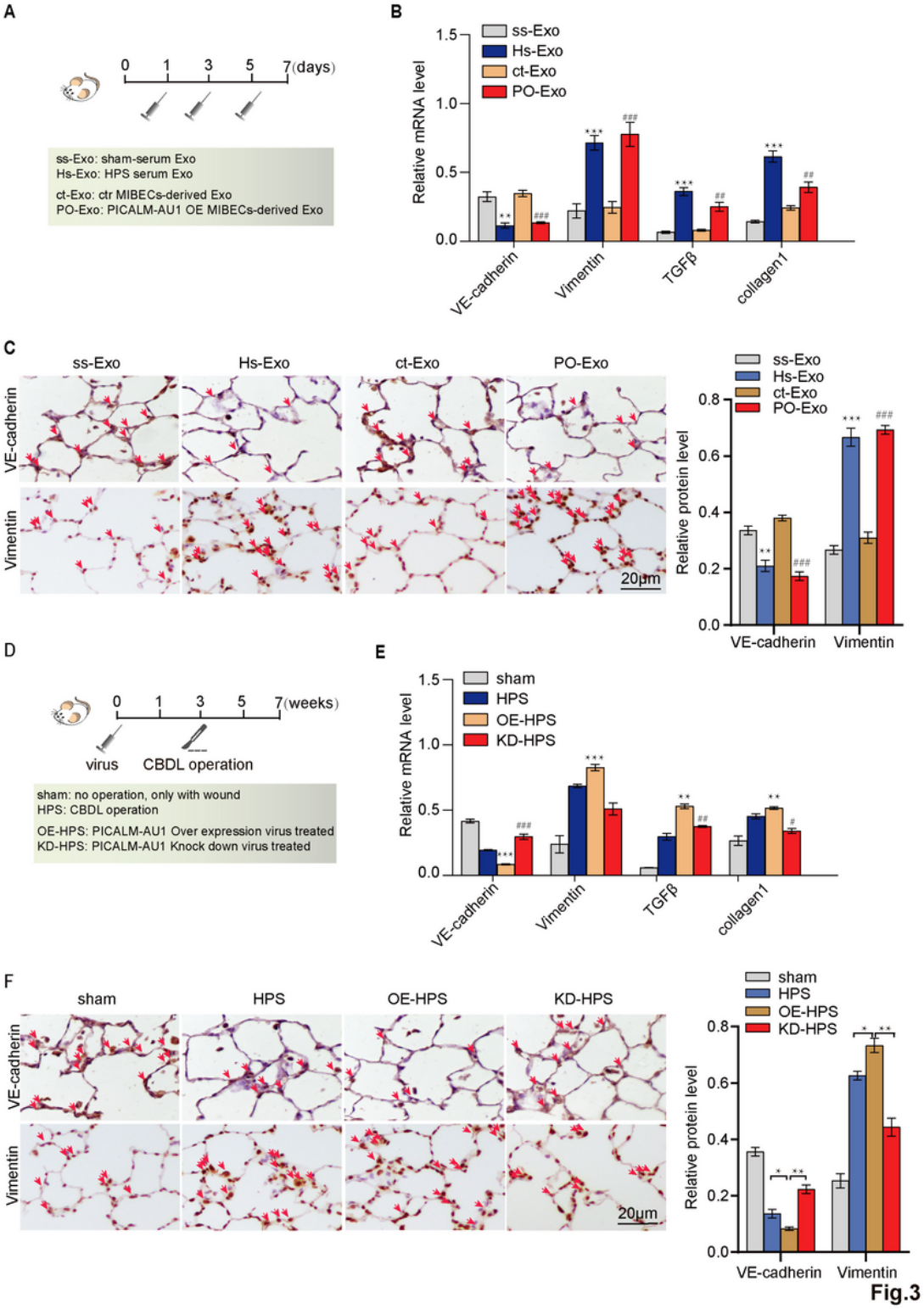

Fig.3

Figure 3

Exo-PICALM-AU1 promoted PMVECs EndMT (A) Experimental protocol of exosomes treated rat. (B) Relative mRNA level was detected by qPCR. Statistical significance relative to ss-Exo treated group, *P < 0.05, **P < 0.01, ***P < 0.001; relative to ct-Exo treated group, #P < 0.05, ##P < 0.01, ###P < 0.001, n=5. (C) IHC showed endothelia cell marker (VE-cadherin) expressed reduce and mesenchymal cell marker (Vimentin) expressed induced during the HPS rat lung; (ss-Exo, Serum exosomes from sham rat; HPS-Exo, serum exosomes from 3-week CBDL rat; ct-Exo, exosomes from the culture medium of control MIBECs cells; PO-Exo, exosomes from PICALM-AU1 over expression MIBECs cells). (left, IHC staining; Right, Quantification of related proteins). (D) Experimental protocol of PICALM-AU1 over expression and knockdown in HPS rat. (E) Relative mRNA level was detected by qPCR. Statistical significance relative to sham group, *P < 0.05, **P < 0.01, ***P < 0.001; relative to HPS group, #P < 0.05, ##P < 0.01, ###P < 0.001, n=5. Data were compared by 2-way ANOVA. (F) IHC showed endothelia cell marker (VE-cadherin) expressed reduce and mesenchymal cell marker (Vimentin) expressed induced during the HPS rat lung. (left, IHC staining; Right, Quantification of related proteins).

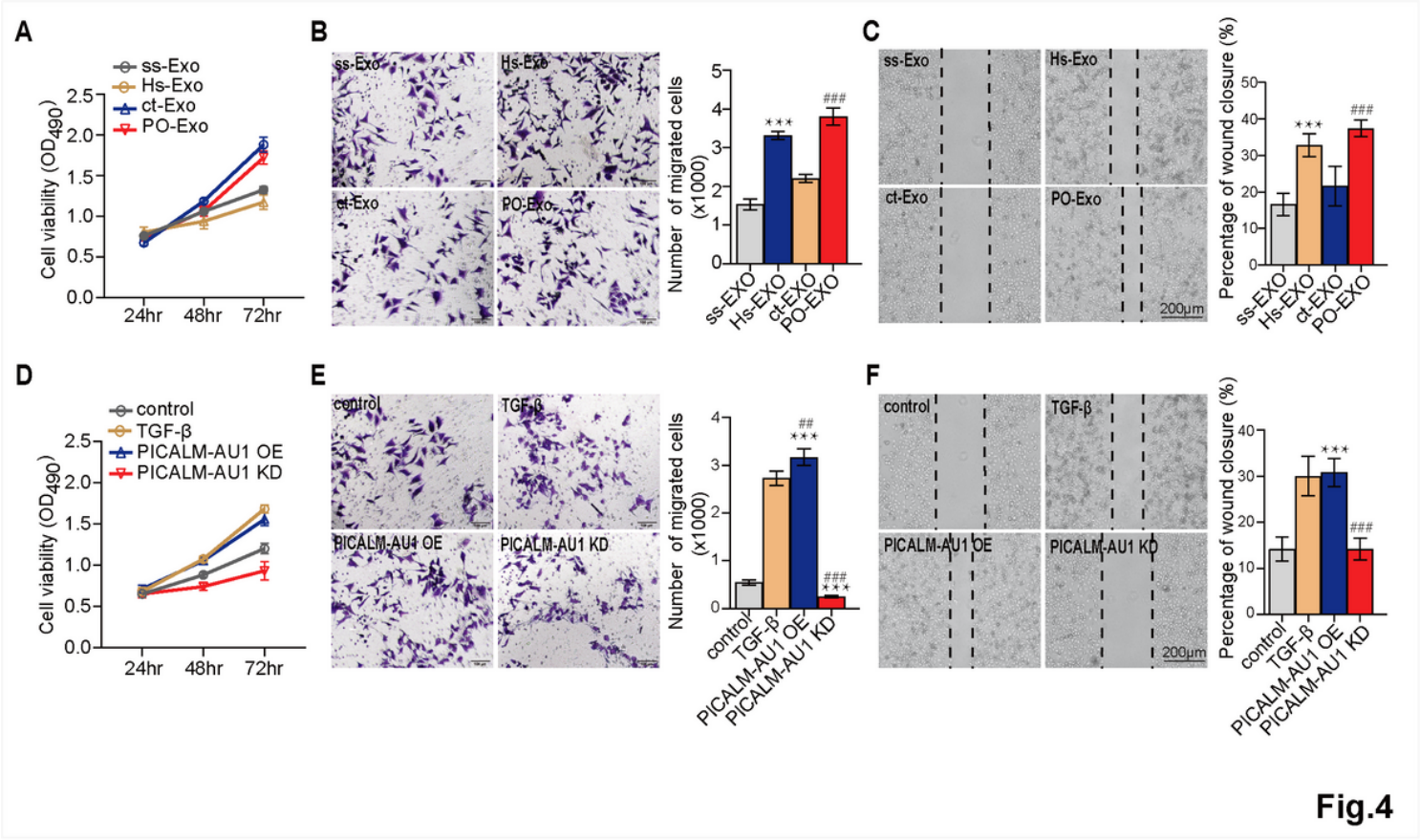

Fig.4

Figure 4

Exo-PICALM-AU1 promoted PMVECs proliferation and migration (A-C) Exosomes treated PMVECs cell. HPS rat serum derived exosome and Over expression MIBECs cells derived exosome induce PMVECs proliferation (A) and migration (B, C), statistical significance relative to ss-Exo treated group, *P < 0.05, **P < 0.01, ***P < 0.001; relative to ct-Exo treated group, #P < 0.05, ##P < 0.01, ###P < 0.001, n = 5. (D-F)

PICALM-AU1 over expression and knockdown lentivevirus treated PMVECs cell. D, over expression of PICALM-AU1 induce PMVECs proliferation (D) and migration (E, F), PICALM-AU1 knock down reduce PMVECs proliferation and migration. Statistical significance relative to control, *P < 0.05, **P < 0.01, ***P < 0.001; relative to TGFβ, #P < 0.05, ##P < 0.01, ###P < 0.001, n = 5. Data were compared by 2-way ANOVA.

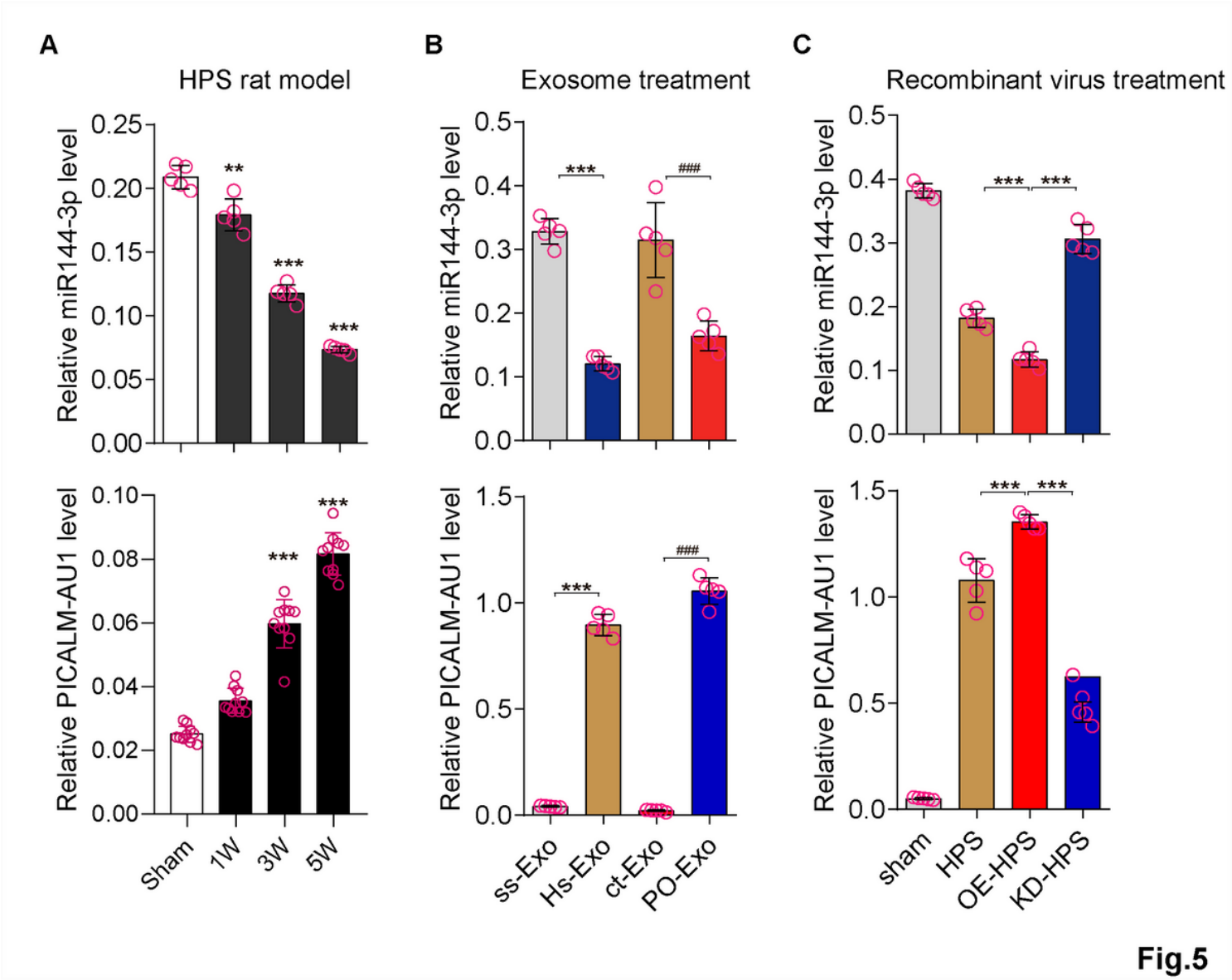

Figure 5

miR144-3p is reduced by PICALM-AU1 (A) The expression trend of miR144-3p and PICALM-AU1 in HPS rat lung; (B) miR144-3p, PICALM-AU1 mRNA level in exosome treatment rat model; (C) miR144-3p, PICALM-AU1 mRNA level in exosome treatment rat model. *P < 0.05, **P < 0.01, ***P < 0.001; #P < 0.05, ##P < 0.01, ###P < 0.001, n = 5. Data were compared by 2-way ANOVA.

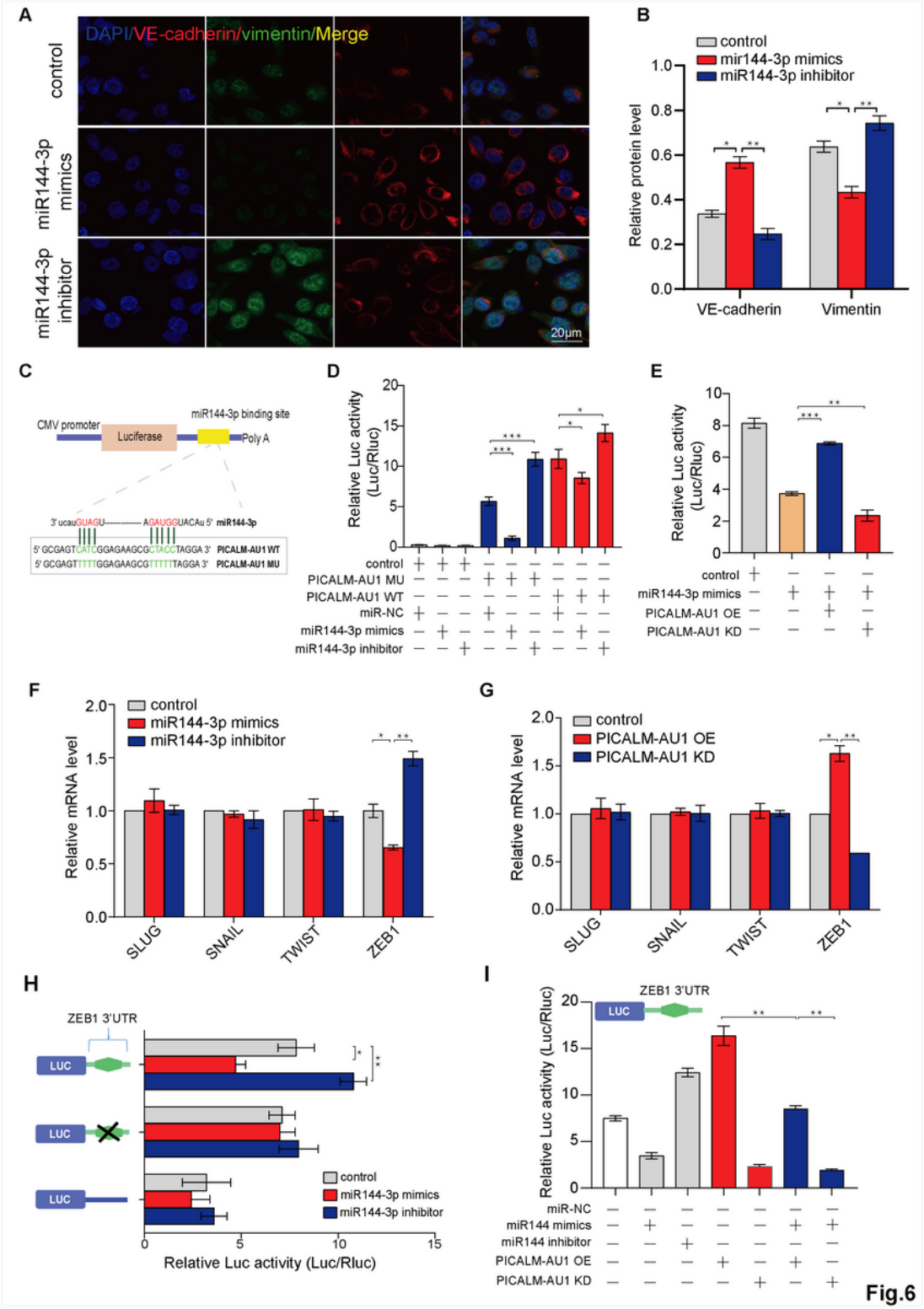

Figure 6

PICALM-AU1 promotes PMVECs EndMT by inhibiting miR144-3p/Zeb1 (A) IF analysis VE-cadherin and vimentin stain in the miR144-3p mimics and inhibitor treatment PMVECs. (B) Quantification of related proteins expression in PMVECs. (C) Schematic outline of predicted binding sites for miR144-3p on Lnc PICALM-AU1. (D) Luciferase activity of psiCHECK2-PICALM-AU1 and psiCHECK2-PICALM-AU1mut upon transfection of indicated miRNA mimics in PMVECs (n=3). psiCHECK2-miR144-3p (3×) was used as

positive control. Data are presented as the ratio of Renilla luciferase activity to Firefly luciferase activity. (E) Luciferase activity of psiCHECK2-PICALM-AU1 upon PICALM-AU1 overexpression or knock down lentive virus treated PMVECs. (F) qPCR analysis key EndMT relative transcriptional factors expression after miR144-3p up-regulated and down-regulated in PMVECs. (G) qPCR analysis key EndMT relative transcriptional factors expression by PCALM-AU1 up-regulated and down-regulated in PMVECs. (H) Dure luciferances assay analysis miR144-3p inhibit ZEB1 expression. (I) Dure luciferances assay analysis PICALM-AU1 regulated miR144-3p/ ZEB1 expression.

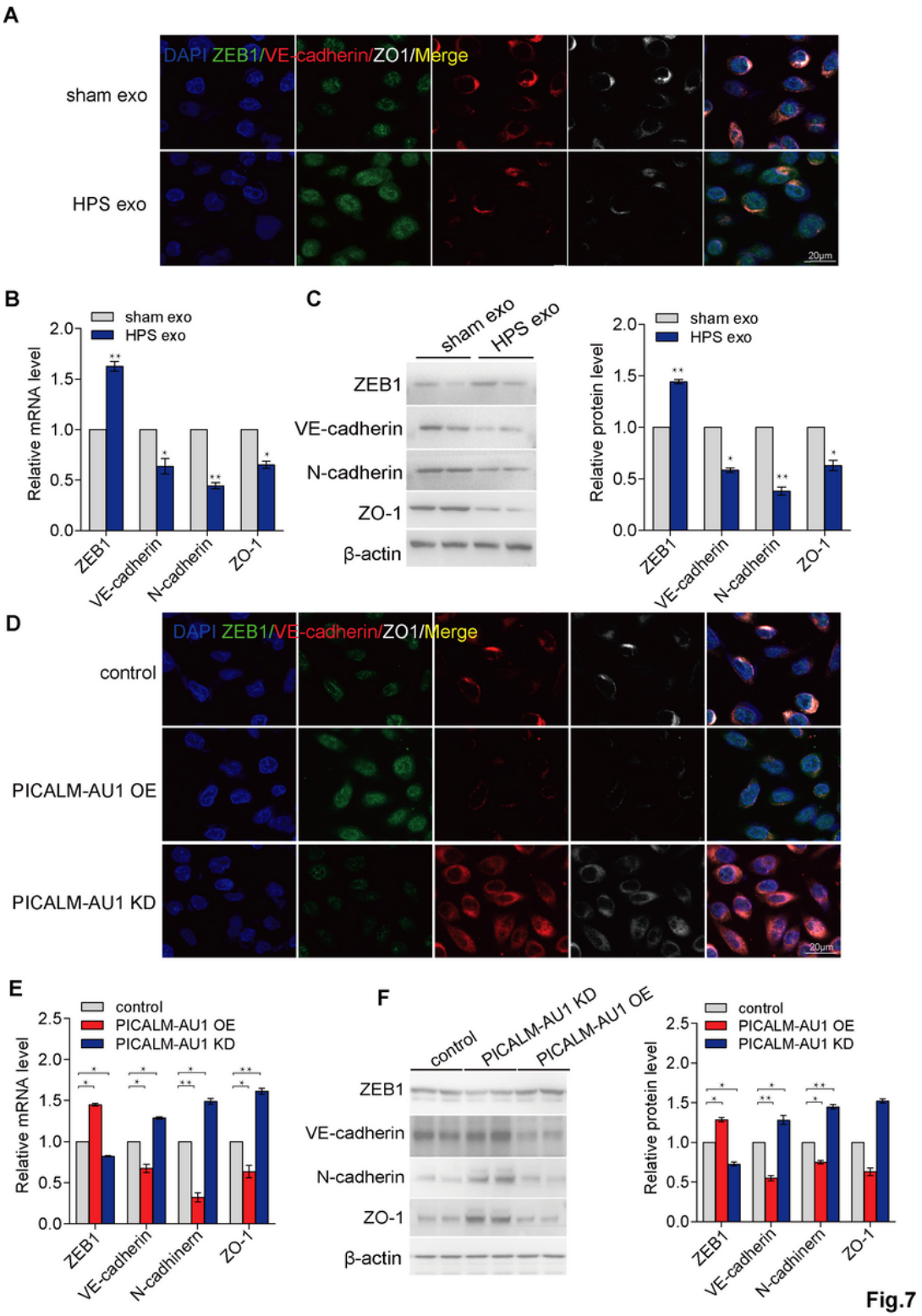

Fig.7

Figure 7

PICALM-AU1 induced PMVECs EndMT by inhibiting miR144-3p/ZEB1 (A-C) IF, qPCR and Western blot showed ZEB1 expression was induced and VE-cadherin and ZO-1 expression was reduced after HPS exosome treatment than that of sham exosome treatment; (D-F) IF, qPCR and Western blot showed ZEB1 expression was induced and VE-cadherin, ZO-1 expression was reduced after PICALM-AU1 over expression than that of control. And ZEB1 expression was reduced and VE-cadherin, ZO-1 expression was induced after PICALM-AU1 knockdown than that of control.

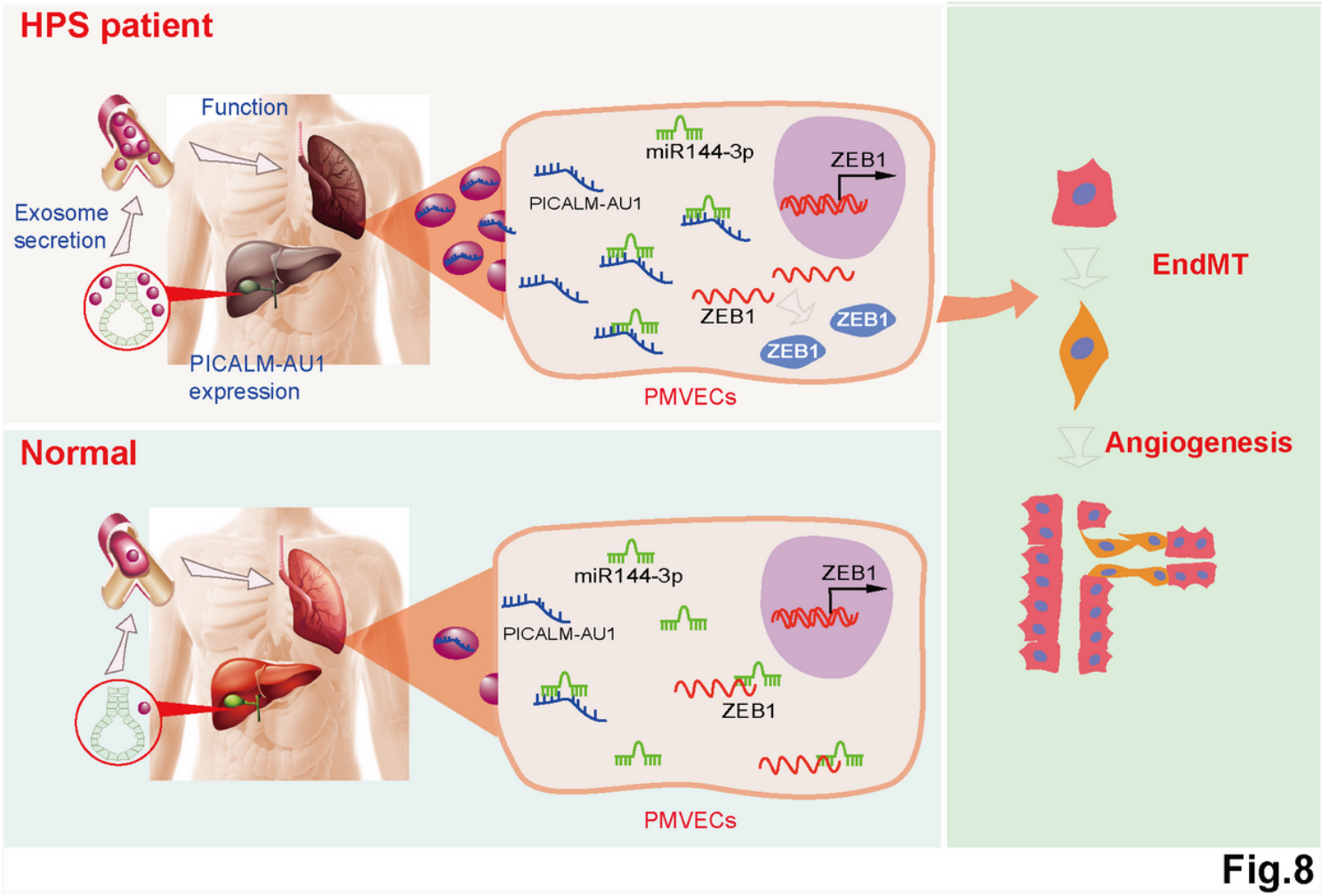

Figure 8

Schematic showing the model of PICALM-AU1 in HPS Hepatocytes secrete exosomes containing PICALM-AU1 in HPS, and then transmitted into the PMVECs. Functionally, exosomal PICALM-AU1 promotes EndMT and pathological angiogenesis in HPS lung by inducing ZEB1 expression

Supplementary Files

This is a list of supplementary files associated with this preprint. Click to download.

- Table1.HPSclinicaldata.xlsx

- Supplementaryfigures.pdf
- TableS2Antibodiesinformation.xlsx
- TableS1.Primerdesign.xlsx
- TableS3.Predictionofmir144target.xlsx